

# ChemComm

Accepted Manuscript

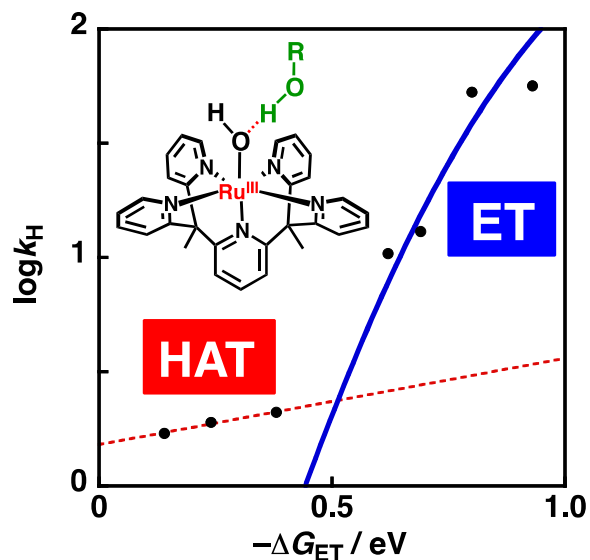


This is an *Accepted Manuscript*, which has been through the Royal Society of Chemistry peer review process and has been accepted for publication.

*Accepted Manuscripts* are published online shortly after acceptance, before technical editing, formatting and proof reading. Using this free service, authors can make their results available to the community, in citable form, before we publish the edited article. We will replace this *Accepted Manuscript* with the edited and formatted *Advance Article* as soon as it is available.

You can find more information about *Accepted Manuscripts* in the [Information for Authors](#).

Please note that technical editing may introduce minor changes to the text and/or graphics, which may alter content. The journal's standard [Terms & Conditions](#) and the [Ethical guidelines](#) still apply. In no event shall the Royal Society of Chemistry be held responsible for any errors or omissions in this *Accepted Manuscript* or any consequences arising from the use of any information it contains.



A mononuclear  $\text{Ru}^{\text{III}}\text{-OH}$  complex oxidizes substrates such as hydroquinones in water through a pre-equilibrium process based on adduct formation by hydrogen bonding between the  $\text{Ru}^{\text{III}}\text{-OH}$  complex and the substrates. The reaction mechanism switches from hydrogen atom transfer to electron transfer depending on the oxidation potentials of substrates.

---

## COMMUNICATION

# Reactivity of a Ru(III)-Hydroxo Complex in Substrate Oxidations in Water†

Cite this: DOI: 10.1039/x0xx00000x

Shingo Ohzu,<sup>a</sup> Tomoya Ishizuka,<sup>a</sup> Hiroaki Kotani<sup>a</sup> and Takahiko Kojima\*<sup>a</sup>

Received 00th January 2012,

Accepted 00th January 2012

DOI: 10.1039/x0xx00000x

www.rsc.org/

A mononuclear Ru<sup>III</sup>-OH complex oxidizes substrates such as hydroquinones in water through a pre-equilibrium process based on adduct formation by hydrogen bonding between the Ru<sup>III</sup>-OH complex and the substrates. The reaction mechanism switches from hydrogen atom transfer to electron transfer depending on the oxidation potentials of substrates.

Substrate oxidation reactions of organic substrates with iron(III)- or other trivalent metal-hydroxo complexes have been intensively investigated due to not only relevance to the active species in biological oxidations catalysed by lipoxygenases<sup>1</sup> but also interests in the high reactivity despite the relatively low oxidation state of the metal centers.<sup>2</sup> The oxidation reactions with synthetic metal(III)-hydroxo complexes as oxidants have been mainly performed in organic solvents.<sup>2-4</sup> In contrast, the reactivity of trivalent metal-hydroxo complexes for substrate oxidations in water has yet to be clarified. Additionally, it has not been well elucidated so far how the reorganization energy ( $\lambda$ ) of electron transfer (ET) for a metal complex affects the reactivity in substrate oxidation performed by the metal complex.<sup>5</sup>

High-valent ruthenium complexes have also been intensively investigated as active species of substrate oxidation reactions both in organic solvents<sup>6</sup> and water.<sup>7</sup> Ruthenium complexes exhibit highly reversible redox behaviours to exhibit high catalytic turnover numbers. The valences of the ruthenium centres of the oxidants employed so far are +IV<sup>8</sup> for most cases, +V<sup>9</sup> or +VI<sup>10</sup> for several cases, whereas there are few reports on a Ru<sup>III</sup>-hydroxo complex as an active species for substrate oxidation in water. Herein, we report detailed kinetic studies on substrate oxidation reactions with a Ru<sup>III</sup>-hydroxo complex in water (Fig. 1).

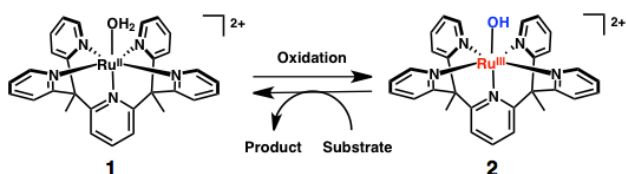


Fig. 1 Generation of [Ru<sup>III</sup>(OH)(PY5Me<sub>2</sub>)]<sup>2+</sup> (2) from [Ru<sup>II</sup>(PY5Me<sub>2</sub>)(H<sub>2</sub>O)]<sup>2+</sup> (1) and oxidation of substrates with 2.

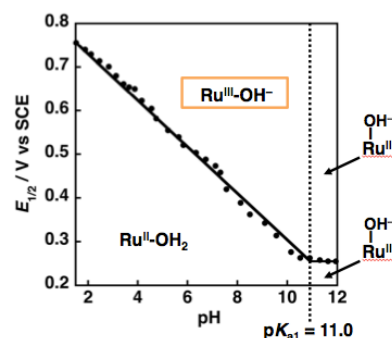


Fig. 2 A plot of redox potentials against solution pH (Pourbaix diagram) for **1** in B.-R. buffer. Potentials were determined relative to SCE (as 0 V) at room temperature.

A Ru<sup>II</sup>-aqua complex with a pentadentate poly-pyridyl ligand, 2,6-bis{1,1-bis(2-pyridyl)ethyl}pyridine (PY5Me<sub>2</sub>),<sup>11</sup> [Ru<sup>II</sup>(PY5Me<sub>2</sub>)(OH<sub>2</sub>)]<sup>2+</sup> (**1**), was synthesized by treatment of [Ru<sup>II</sup>Cl(PY5Me<sub>2</sub>)]<sup>+</sup> (see Figs S1 and S2 in Electronic Supplementary Information (ESI)) with AgPF<sub>6</sub> in water. Characterization of **1** was made by using <sup>1</sup>H NMR spectroscopy, ESI-TOF-MS spectrometry and elemental analysis.<sup>12</sup> The  $pK_a$  values of **1** were determined in Britton-Robinson (B.-R.) buffer<sup>13</sup> based on the UV-Vis spectral change (Fig. S3 in ESI) to be  $pK_{a1} = 11.0$ . Cyclic and differential-pulse voltammograms (CV and DPV) of **1** were measured in B.-R. buffer at various pH and the Pourbaix diagram was drawn based on the results of the electrochemical measurements and the  $pK_a$  values determined (Fig. 2). In the pH range and within the potential window measured, no wave due to a Ru<sup>III</sup>/Ru<sup>IV</sup> redox couple was observed (Fig S4 in ESI). In the Pourbaix diagram, the potential of the oxidation step decreases as the solution pH increases with an inclination of  $-52$  mV/pH in the pH range of 1.8–11.0. The result indicates the  $1e^-$  and  $1H^+$  process of the Ru<sup>II</sup>-OH<sub>2</sub> to give complex **2** in the pH range. The BDE value of **1** was estimated to be 77 kcal mol<sup>-1</sup>, on the basis of the redox potential and the  $pK_a$  value.<sup>12</sup>

Electrochemical oxidation of **1** (0.5 mM) at +1.3 V vs SCE in B.-R. buffer (pH 1.8) clearly exhibited the one-step spectral change due to generation of **2** (Fig. S5 in ESI). The UV-Vis spectral change in the course of the electrochemical oxidation of **1** ended at the

elementary electric charges of 0.097 C, which matched with the theoretical value for the one-electron oxidation of the Ru<sup>II</sup> species to form the corresponding Ru<sup>III</sup> complex (0.093 C). The ESI-MS spectrum was measured for the aqueous solution of **2** generated by the electrochemical oxidation of **1** and a peak cluster was observed at  $m/z = 281.17$  with the feature of a divalent cation, which was ascribable to the signal of  $[2 - 2PF_6]^{2+}$  (Fig. S6 in ESI).

To elucidate the reactivity of **2** in oxidations of organic substrates, we performed kinetic analyses on the quantitative oxidation of 2,5-chlorohydroquinone (H<sub>2</sub>QCl<sub>2</sub>) with electrochemically generated **2**.<sup>14</sup> The reactions were performed in the presence of an excess amount of H<sub>2</sub>QCl<sub>2</sub> (25–150 mM) relative to **2** (0.5 mM) in B.-R. buffer (pH 1.8) and the rate constants were determined by UV/Vis spectroscopy to trace the rise of absorption due to the Ru<sup>II</sup> species at 380 nm at various temperatures (Fig. 3a). All the time courses of the absorbance changes obeyed first-order kinetics and the pseudo-first-order rate constants ( $k_{\text{obs}}$ ) were determined under various concentrations of H<sub>2</sub>QCl<sub>2</sub>. In the oxidation of H<sub>2</sub>QCl<sub>2</sub> with **2**, the pseudo-first-order rate constants were saturated against the concentration of H<sub>2</sub>QCl<sub>2</sub> at all the temperatures examined (Fig. 3b and Fig. S8 in ESI), indicating the existence of pre-equilibrium processes prior to the oxidation.<sup>7</sup>

We also made kinetic analyses for oxidations of two more substrates, 2,3,5,6-tetrafluoro-hydroquinone (H<sub>2</sub>QF<sub>4</sub>) and ascorbic acid (AS). The kinetic analyses for oxidations of the three substrates allowed us to determine the equilibrium constants ( $K$ ) for the pre-equilibrium processes and the first-order rate constants ( $k$ ) at various temperatures (Fig. S8 in ESI). Based on the plots of the equilibrium constants and the rate constants relative to the inverse of the reaction temperatures ( $T^{-1}$ ) (van't Hoff plots and Eyring plots, respectively), the thermodynamic parameters for the pre-equilibrium processes and the activation parameters for the oxidation reactions were determined respectively (Table 1 and Figs. S9 and S10 in ESI). The enthalpy changes ( $\Delta H^\circ$ ) of the pre-equilibrium process show

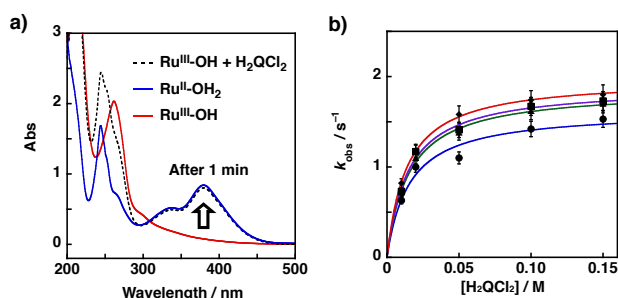


Fig. 3 (a) Spectral changes during the oxidation of H<sub>2</sub>QCl<sub>2</sub> with **2** (0.5 mM) in B.-R. buffer (pH 1.8): at 297 K. The initial spectrum of **2** before adding the substrate (red) and the final spectrum after the oxidation reaction (black dotted line) and the spectrum of **1** (blue) are shown. (b) Pseudo-first-order kinetic analysis for the oxidation of H<sub>2</sub>QCl<sub>2</sub> with **2** as oxidant (0.5 mM) in B.-R. buffer (pH 1.8) at 305 (red), 297 (purple), 289 (green), and 281 K (blue).

Table 1 Oxidation potentials and thermodynamic parameters for the pre-equilibrium processes and activation parameters for the oxidation reactions of substrates with **2**

substrate	$E_{\text{ox}}^a$	$\text{p}K_{\text{a}1}$	$\Delta H^\circ{}^b$	$\Delta S^\circ{}^c$	$\Delta H^\circ{}^b$	$\Delta S^\circ{}^c$
H <sub>2</sub> QF <sub>4</sub>	+0.61	3.90	8.0	-18	-7.6	10
H <sub>2</sub> QCl <sub>2</sub>	+0.51	4.96	4.0	-28	-4.2	20
AS	+0.37	5.17	12	1.4	-1.4	22
H <sub>2</sub> QCl	+0.06	9.21	6.6	-3.4	1.3	27
H <sub>2</sub> QF	+0.13	9.42	6.1	-7.3	1.7	27
H <sub>2</sub> Q	-0.05	9.95	7.4	10.5	1.4	26

<sup>a</sup> V vs SCE. <sup>b</sup> kJ mol<sup>-1</sup>. <sup>c</sup> J mol<sup>-1</sup> K<sup>-1</sup>.

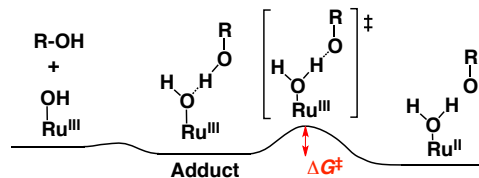


Fig. 4 Schematic energy diagram of the intermediates for the substrate oxidation with **2** in water. R represents aryl or alkyl groups of the substrates.

tendency to become more negative with increasing the acidity of the hydroxy groups of substrates,<sup>15,16</sup> indicating hydrogen bonding between the oxygen of **1** and the hydroxy group of a substrate as the driving force of the adduct formation. In addition, the relatively small activation parameters suggest that the pre-equilibrium process between **2** and the substrate afforded appropriate arrangement for hydrogen-atom transfer (HAT) (Fig. 4).

To obtain further information on the oxidation process, studies of the kinetic isotope effects (KIE) for oxidation reactions of substrates with **2** were conducted at 297 K. The KIE values were determined as the ratio of the rate constants ( $k_{\text{H}}/k_{\text{D}}$ ) for the oxidation reactions of substrates using H<sub>2</sub>O ( $k_{\text{H}}$ ) and D<sub>2</sub>O ( $k_{\text{D}}$ ) as solvents (Fig. S11 in ESI). The reactions were monitored by UV-Vis spectroscopy to track the rise of the absorbance due to the Ru<sup>II</sup> species formed. The oxidations of substrates showed KIE values for the hydroxy group to be 1.7 for H<sub>2</sub>QCl<sub>2</sub> and H<sub>2</sub>QF<sub>4</sub>, and 1.2 for AS (Table 2).<sup>17</sup> The KIE values for oxidations with the three substrates indicate that the hydrogen atom abstraction from the hydroxy group is involved in the rate-determining step.

Four more substrates, hydroquinone (H<sub>2</sub>Q), 2-chloro-hydroquinone (H<sub>2</sub>QCl), 2-fluoro-hydroquinone (H<sub>2</sub>QF), and 2-methoxy-hydroquinone (H<sub>2</sub>Q(OMe)), having lower redox potentials (-0.05 V vs SCE for H<sub>2</sub>Q, +0.06 V for H<sub>2</sub>QCl, +0.13 V for H<sub>2</sub>QF, -0.18 V for H<sub>2</sub>Q(OMe)) than those of other three substrates (+0.51 V for H<sub>2</sub>QCl<sub>2</sub> and +0.61 V for H<sub>2</sub>QF<sub>4</sub> and +0.37 V for AS vs SCE), were utilized as substrates for the oxidation reactions with **2** (Fig. S12 in ESI).<sup>14</sup> The three substrates also exhibited the pre-equilibrated adduct formation (Fig. S8 in ESI) and the  $\Delta H^\circ$  values also showed the similar dependence on the  $\text{p}K_{\text{a}1}$  values of the substrates (Table 1). The larger rate constants for the oxidation of H<sub>2</sub>Q, H<sub>2</sub>QF and H<sub>2</sub>QCl compared to those for the oxidation of the other three substrates probably derive from the lower redox potentials of substrates (Table 1 and Fig. S8 in ESI). In addition, the oxidation reactions of H<sub>2</sub>Q, H<sub>2</sub>QF, H<sub>2</sub>QCl and H<sub>2</sub>Q(OMe) exhibited no KIE (1.1 for H<sub>2</sub>Q, 1.0 for H<sub>2</sub>QCl, 1.1 for H<sub>2</sub>QF, 1.1 for H<sub>2</sub>Q(OMe)), and see Fig. S11 in ESI), indicating that the oxidation reactions of the four substrates proceed through electron transfer (ET) from substrates to **2**.<sup>5</sup>

A plot of the logarithm of the rate constants at 297 K relative to the driving force of ET ( $-\Delta G_{\text{ET}}$ ) was made to shed light on the change of the reaction mechanism from HAT to ET in the substrate oxidation reactions by **2** (Table S1 in ESI). As shown in Fig. 5, substrates giving smaller  $-\Delta G_{\text{ET}}$  (< 0.5 eV) are oxidized in the HAT

Table 2. Kinetic data for oxidation reactions with **2** in B.-R. buffer at 297 K

substrate	$k_{\text{H}}, \text{s}^{-1}$	$k_{\text{D}}, \text{s}^{-1}$	$k_{\text{H}}/k_{\text{D}}$
H <sub>2</sub> Q(OMe)	56	52	1.1
H <sub>2</sub> Q	53	48	1.1
H <sub>2</sub> QCl	13	13	1.0
H <sub>2</sub> QF	10	8.8	1.1
H <sub>2</sub> QCl <sub>2</sub>	1.9	1.1	1.7
H <sub>2</sub> QF <sub>4</sub>	1.7	1.0	1.7
AS	2.1	1.7	1.2

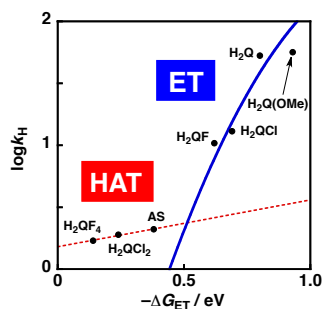


Fig. 5 A plot of the logarithm of rate constants relative to the driving forces of ET ( $-\Delta G_{ET}$ ). All the data were determined at 297 K in B.-R. buffer (pH 1.8). The blue line is drawn by using eq 3 in ESI with  $\lambda = 1.31$  eV and the red dashed line indicates a linear dependence of  $\log k_H$  on  $-\Delta G_{ET}$  for HAT reactions.

mechanism with small driving-force dependence. In stark contrast, those having larger  $-\Delta G_{ET}$  ( $> 0.5$  eV) are oxidized in the ET mechanism and the rate constants fit a Marcus plot<sup>18</sup> for intramolecular non-adiabatic ET with  $\lambda$  of 1.31 eV and the electronic coupling matrix element ( $V$ ) of  $0.0011 \text{ cm}^{-1}$ .<sup>12</sup> The switching point of the reaction mechanisms is estimated to be located at  $-\Delta G_{ET} = 0.51$  eV. The  $\lambda$  value and the  $-\Delta G_{ET}$  of the switching point for the reaction mechanisms of substrate oxidation with **2** is larger than those of other high-valent metal complexes that are proposed to oxidize substrates through ET.<sup>5</sup> These results indicate that the  $\lambda$  value becomes larger and ET from substrates to an oxidant becomes more difficult to occur in a polar solvent like water.<sup>19</sup>

In conclusion, we have synthesized a novel  $\text{Ru}^{\text{III}}\text{-OH}$  complex, **2**, with  $\text{PY5Me}_2$  as a pentadentate polypyridyl ligand by electrochemical oxidation of the corresponding  $\text{Ru}^{\text{II}}\text{-aqua}$  complex in B.-R. buffer. We have experimentally elucidated the reactivity of a  $\text{Ru}^{\text{III}}\text{-OH}$  complex in substrate oxidations in water on the basis of kinetic analysis. The oxidation reactions of substrates by **2** in water involve a pre-equilibrium process based on adduct formation by hydrogen bonding between the  $\text{Ru}^{\text{III}}\text{-OH}$  complex and the substrates.<sup>20</sup> The oxidation reaction mechanism with **2** in water switches from HAT to ET, depending on the oxidation potentials of substrates employed. The switching of the reaction mechanisms for substrate oxidation reactions has never been observed without assistance by Lewis-acidic metal ions to control the reduction potential of the oxidant.<sup>5</sup> The point to observe the mechanistic switching here is the remarkable increase of the  $\lambda$  value of ET in water, which enables the slow ET from substrates showing positive  $-\Delta G_{ET}$ . This work may provide a valuable basis to elucidate the reactivity of a trivalent metal-hydroxo complex in oxidation reactions of organic substrates in water in relevance to those catalysed by lipoxygenases.

## Notes and references

<sup>a</sup> Department of Chemistry, Faculty of Pure and Applied Sciences, University of Tsukuba, 1-1-1 Tennoudai, Tsukuba, Ibaraki 305-8571, Japan. E-mail: kojima@chem.tsukuba.ac.jp

<sup>†</sup> Electronic Supplementary Information (ESI) available: Experimental details of syntheses and characterization of compounds, summary of optical absorption and redox potentials, cyclic and differential-pulse voltammograms. CCDC-1022568 contains the supplementary crystallographic data. See DOI: 10.1039/c000000x/

1 (a) T. M. Jonsson, H. Glickman, S. J. Sun and J. P. Klinman, *J. Am. Chem. Soc.*, 1996, **118**, 10319; (b) C.-C. Hwang and C. B. Grissom,

*J. Am. Chem. Soc.*, 1994, **116**, 795; (c) E. R. Lewis, E. Johansen and T. R. Holman, *J. Am. Chem. Soc.*, 1999, **121**, 1395.

- 2 (a) C. R. Goldsmith and T. D. P. Stack, *Inorg. Chem.*, 2006, **45**, 6048; (b) C. R. Goldsmith, A. P. Cole and T. D. P. Stack, *J. Am. Chem. Soc.*, 2005, **127**, 9904.
- 3 P. J. Donoghue, J. Tehranchi, C. J. Cramer, R. Sarangi, E. I. Solomon and W. B. Tolman, *J. Am. Chem. Soc.*, 2011, **133**, 17602.
- 4 (a) C. R. Goldsmith and T. D. P. Stack, *Inorg. Chem.*, 2006, **45**, 6048; (b) C. R. Goldsmith, A. P. Cole and T. D. P. Stack, *J. Am. Chem. Soc.*, 2005, **127**, 9904.
- 5 (a) Y. Morimoto, J. Park, T. Suenobu, Y.-M. Lee, W. Nam and S. Fukuzumi, *Inorg. Chem.*, 2012, **51**, 10025; (b) J. Park, Y. Morimoto, Y.-M. Lee, W. Nam and S. Fukuzumi, *J. Am. Chem. Soc.*, 2011, **133**, 5236; (c) J. Park, Y. Morimoto, Y.-M. Lee, W. Nam and S. Fukuzumi, *Inorg. Chem.*, 2014, **53**, 3618.
- 6 (a) T. J. Meyer, *Acc. Chem. Res.*, 1989, **22**, 163. (b) S. L.-F. Chan, Y.-H. Kan, K.-L. Yip, J.-S. Huang and C.-M. Che, *Coord. Chem. Rev.*, 2011, **255**, 899; (c) M. Zhou and R. H. Crabtree, *Chem. Soc. Rev.*, 2011, **40**, 1875.
- 7 (a) T. Ishizuka, S. Ohzu and T. Kojima, *Synlett*, 2014, **25**, 1667; (b) Y. Hirai, T. Kojima, Y. Mizutani, Y. Shiota, K. Yoshizawa and S. Fukuzumi, *Angew. Chem., Int. Ed.*, 2008, **47**, 5772; (c) T. Kojima, Y. Hirai, T. Ishizuka, Y. Shiota, K. Yoshizawa, K. Ikemura, T. Ogura and S. Fukuzumi, *Angew. Chem., Int. Ed.*, 2010, **49**, 8449; (d) S. Ohzu, T. Ishizuka, Y. Hirai, H. Jiang, M. Sakaguchi, T. Ogura, S. Fukuzumi and T. Kojima, *Chem. Sci.*, 2012, **3**, 3421.
- 8 (a) W. K. Seok and T. J. Meyer, *J. Am. Chem. Soc.*, 1988, **110**, 7358; (b) P. Neubold, K. Wiegardt, B. Nuber and J. Weiss, *Angew. Chem., Int. Ed. Engl.*, 1988, **27**, 933.
- 9 (a) M. M. T. Khan, D. Chatterjee, R. R. Merchant, P. Paul, S. H. R. Abdi, D. Srinivas, M. R. H. Siddiqui, M. A. Moiz, M. M. Bhadbhade and K. Venkatasubramanian, *Inorg. Chem.*, 1992, **31**, 2711; (b) X. Guan, S. L.-F. Chan and C.-M. Che, *Chem. Asian J.*, 2013, **8**, 2046.
- 10 S. Perrier, T. C. Lau and J. K. Kochi, *Inorg. Chem.*, 1990, **29**, 4190.
- 11 E. A. Ünal, D. Wiedemann, J. Seiffert, J. P. Boyd and A. Grohmann, *Tetrahedron. Lett.*, 2012, **53**, 54.
- 12 See ESI.
- 13 R. Wang, J. G. Vos, R. H. Schmehl and R. Hage, *J. Am. Chem. Soc.*, 1992, **114**, 1964.
- 14 The products of oxidation reactions of hydroquinones were confirmed to be the corresponding quinones by <sup>1</sup>H NMR spectroscopy. See Fig. S7 in ESI.
- 15 X.-Q. Zhu, C.-H. Wang, and H. Liang, *J. Org. Chem.*, 2010, **75**, 7240.
- 16 Y.-N. Wang, K.-C. Lau, W. W. Y. Lam, W.-L. Man, C.-F. Leung and T.-C. Lau, *Inorg. Chem.*, 2009, **48**, 400.
- 17 Small KIE values in HAT reactions have been reported: (a) T. Osako, K. Ohkubo, M. Taki, Y. Tachi, S. Fukuzumi and S. Itoh, *J. Am. Chem. Soc.*, 2003, **125**, 11027; (b) S. C. Weatherly, I. V. Yang and H. H. Thorp, *J. Am. Chem. Soc.*, 2001, **123**, 1236.
- 18 (a) R. A. Marcus and N. Sutin, *Biochim. Biophys. Acta* 1985, **811**, 265; (b) R. A. Marcus, *Angew. Chem., Int. Ed. Engl.*, 1993, **32**, 1111.
- 19 S. Fukuzumi, K. Ohkubo, T. Suenobu, K. Kato, M. Fujitsuka and O. Ito, *J. Am. Chem. Soc.*, 2001, **123**, 8459.
- 20 S. Ohzu, T. Ishizuka, S. Ohzu, H. Kotani, Y. Shiota, K. Yoshizawa and T. Kojima, *Chem. Sci.* 2014, **5**, 1429.